ARTICLE

Impact of Oxygen Vacancy on Band Structure Engineering of n-p Codoped Anatase TiO_2

Qiang-qiang Meng[a], Jia-jun Wang[b], Jing Huang[a,c*], Qun-xiang Li[a*]

a. Hefei National Laboratory for Physical Sciences at the Microscale, University of Science and Technology of China, Hefei 230026, China
b. College of Chemistry, Tianjin Normal University, Tianjin 300387, China
c. School of Materials and Chemical Engineering, Anhui Jianzhu University, Hefei 230601, China

(Dated: Received on November 12, 2014; Accepted on November 18, 2014)

Doping with various impurities is an effective approach to improve the photoelectrochemical properties of TiO_2. Here, we explore the effect of oxygen vacancy on geometric and electronic properties of compensated (*i.e.* V-N and Cr-C) and non-compensated (*i.e.* V-C and Cr-N) codoped anatase TiO_2 by performing extensive density functional theory calculations. Theoretical results show that oxygen vacancy prefers to the neighboring site of metal dopant (*i.e.* V or Cr atom). After introduction of oxygen vacancy, the unoccupied impurity bands located within band gap of these codoped TiO_2 will be filled with electrons, and the position of conduction band offset does not change obviously, which result in the reduction of photoinduced carrier recombination and the good performance for hydrogen production via water splitting. Moreover, we find that oxygen vacancy is easily introduced in V-N codoped TiO_2 under O-poor condition. These theoretical insights are helpful for designing codoped TiO_2 with high photoelectrochemical performance.

Key words: Oxygen vacancy, Band structure engineering, n-p codoped, Anatase TiO_2

I. INTRODUCTION

The development of advanced catalytic materials for energy and environmental applications is an active research area around the world. As a promising photocatalyst for hydrogen production of water splitting, titanium oxide (TiO_2) has received much research attention due to its high photocatalytic activity, resistance to photo-corrosion, low cost, and nontoxicity [1−4]. However, the photo-reaction efficiency of TiO_2 is severely limited by its large intrinsic band gap (*e.g.*, 3.20 eV for the anatase phase), the capability of absorbing in ultraviolet portion of the solar spectrum [5, 6]. A crucial prerequisite for enhancing the solar energy conversion efficiency is to enable TiO_2 to absorb more abundant visible light by reducing its band gap below 2.0 eV [7−9].

Till now, many attempts have been made to optimize the band gap of TiO_2 by diffierent methods [7−11]. Doping with various elements including non-metals [10, 11] and transition metals [12, 13] would be promising ways to optimize the band gaps and enhance the visible light photo-catalytic activity of TiO_2. However, the photoelectochemical efficiency of these non-metal and transition metals doped TiO_2 is still limited by a relative high electron-hole recombination rate, resulting the loss of photo-generated electron-hole pairs [14, 15]. To avoid these problems, two most important theoretical concepts have been well established. One is the compensated n-p codoping approach, which does not change the basic electronic structures of the host lattice, but generates dopant levels at the band edges [7]. The other is non-compensated n-p codoping approach, which ensures the creation of intermediate bands within the band gap, and effectively narrow the band gap [8, 9].

Note that the photoelectrochemical properties of TiO_2, such as light absorption, photocatalytic reactivity and selectivity, can be modulated by the always existing defects [16−18]. For example, oxygen vacancy is one of the most important and prevalent defects in metal oxides [19], which have been extensively investigated by both theoretical calculations and experimental characterizations [20, 21]. Previous investigations have revealed that the band structures, the electron-hole recombination process as well as the photoelectrical properties of TiO_2 can be effectively tuned by oxygen vacancies which will lead to an unpaired electron in the primitive cell, and in the absence of additional defects will turn the material into a conductor [22]. Unfortunately, no theoretical effort has been made to explore the impact arising from oxygen vacancy on the electronic properties of n-p codoped TiO_2. Here, we perform extensive density functional theory (DFT) calculations to investigate the geometry structures, formation

*Authors to whom correspondence should be addressed. E-mail: jhuang@ustc.edu.cn, liqun@ustc.edu.cn

energies and electronic properties of the n-p codoped anatase TiO_2 with oxygen vacancy. The calculated results clearly reveal that oxygen vacancy prefers to occupy the neighboring site of metal dopant (*i.e.* V and Cr atom). Upon the introduction of oxygen vacancy, these unoccupied impurity bands within the band gap in n-p codoped anatase TiO_2 will be filled with electrons, and the alignment of conduction bands in the codoped systems are not sensitive to the presence of oxygen vacancy, which benefits for hydrogen production via water splitting. We find that oxygen vacancy can be easily introduced in V-N codoped systems under O-poor condition.

II. METHODS AND COMPUTATIONAL DETAILS

The first-principles calculations are performed using the projected augmented wave (PAW) plane-wave basis, implemented in the Vienna *ab initio* simulation package (VASP) [23, 24]. In our calculations, an energy cutoff of 520 eV is employed. The exchange-correlation interaction is treated with the Perdew-Burke-Ernzerhof (PBE) generalized gradient approximation [25]. A 2×2×2 and 4×4×4 Morkhost-Pack k-point mesh is used to sample the Brillouin zone for geometric and electronic structures calculations, respectively [26]. All atomic positions are optimized using the conjugate gradient scheme without any symmetric restrictions until the maximum force on the each of them is less than 0.02 eV/A. It is well known that conventional DFT methods do not accurately predict the positions of these impurity bands within the band gap. To overcome this shortcoming, we used the DFT+U method [27, 28] to treat the 3d electrons of the transition metals with the Hubbard on-site Coulomb interaction. Similar to Anisimov *et al.* report [28], the value of U for Ti, V, and Cr atom is set to be 7.0, 3.0, and 3.0 eV, respectively.

To examine these n-p co-doped anatase TiO_2 systems with oxygen vacancy, a 3×3×1 supercell with 108 atoms (36 Ti and 72 O atoms) is adopted, as shown in Fig.1(a). Here, the n and p-type dopants substitute Ti and O sites in TiO_2, which are labeled with cyan and gray colors, respectively. The optimized lattice parameters (a and c) of pure TiO_2 are predicted to be 3.82 and 9.69 Å, which are close to the previous experimental and theoretical values [29].

III. RESULTS AND DISCUSSION

A. Formation energy and optimized structure

We first determine the location of oxygen vacancy in TiO_2 codoped with four different n-p pairs. In these systems, the dopants are introduced into anatase TiO_2 by replacing a host Ti atom with an n-type dopant (*i.e.* V or Cr atom), and a neighboring O atom with a p-type

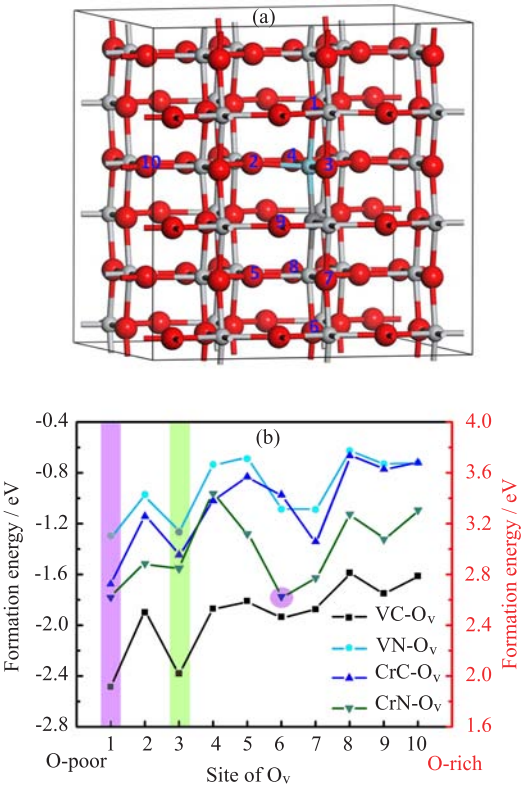

FIG. 1 (a) Computational model for the n-p codoped TiO_2 with oxygen vacancy. The location of oxygen vacancy in a 3×3×1 supercell is labeled with numbers from 1 to 10. The gray and red balls stand for Ti and O atoms, respectively and the colour balls labeled on the Ti and O atoms are used to illustrate the doped sites. (b) The calculated relative formation energy for these n-p codoped TiO_2 with oxygen vacancy as a function of the O-poor and O-rich chemical potentials, the most stable and metastable sites for oxygen vacancy are labeled with the purple and green shadow areas, respectively.

dopant (*i.e.* C or N atom). It has been revealed that two n-type and p-type dopants prefer to form a pair occupying neighboring lattice sites [8]. That is to say, we examine the net p-type (V-C), the net n-type (Cr-N), and the compensated (V-N and Cr-C) codoped TiO_2 systems with oxygen vacancy. Before examining the geometric and electronic structures of these codoped TiO_2 with oxygen vacancy, we perform test calculation for these codoped TiO_2 to check the accuracy of our procedure. The obtained band structures are similar to these reported in Refs.[7, 8].

To find the energetically preferred site of oxygen vacancy in these codoped systems, we define the formation energy ($E_{\rm form}$) as

$$E_{\rm form} = E_{\rm TiO_2^{np+O_v}} - E_{\rm TiO_2^{np}} + \mu_{\rm O} \qquad (1)$$

here, $E_{\rm TiO_2^{np+O_v}}$ and $E_{\rm TiO_2^{np}}$ stand for the total energies of these n-p codoped TiO_2 with or without oxygen vacancy, $\mu_{\rm O}$ denotes the chemical potential of oxy-

DOI:10.1063/1674-0068/28/cjcp1411196

gen. Clearly, the predicted formation energies for these codoped systems oxygen vacancy vary as a function of μ_O, which depends on the experimental environment.

Namely, the low and high values of μ_O correspond to the O-poor and O-rich conditions, respectively. For pure TiO_2, the μ_{Ti} and μ_O satisfy the relationship: $\mu_{Ti}+2\mu_O=\mu_{TiO_2}$, $\mu_O\leq\mu_{O_2}/2$, and $\mu_{Ti}\leq\mu_{Ti_{bulk}}$. In our calculations, the μ_O in the O-rich growth condition is defined by the binding energy of an isolated O_2 molecule, while μ_{Ti} is determined by $\mu_{TiO_2}-2\mu_O$. In the O-poor growth condition, μ_{Ti} amounts to the binding energy of a Ti atom in its bulk, and the μ_O is calculated from $\mu_O=(\mu_{TiO_2}-\mu_{Ti})/2$ [30, 31].

In this work, we examine ten different sites for oxygen vacancy in these codoped TiO_2, which is labeled with different numbers from 1 to 10 in the supercell, as shown in Fig.1(a). Figure 1(b) presents the calculated formation energies for these examined n-p codoped TiO_2 with oxygen vacancy as a function of μ_O. It is clear that oxygen vacancy prefers to the neighboring site of metal dopant (*i.e.* V or Cr atom). Except the Cr-N codoped case, the next stablest configuration is that oxygen vacancy appears at the position. For clarity, the most stable and the metastable sites for oxygen vacancy are labeled with the purple and green shadow areas in Fig.1(b), respectively. According to the predicted E_{form}, we find that it is easy to induce oxygen vacancy in these codoped TiO_2 systems under O-poor condition. For example, the E_{form} for oxygen vacancy in V-C codoped TiO_2 under O-poor and O-rich growth conditions is predicted to be −2.48 and 1.92 eV, respectively.

The side views of optimized structures are plotted in Fig.2 for the stablest configurations of n-p codoped TiO_2 with oxygen vacancies. In pure TiO_2, as shown in Fig.2(a), each Ti atom is coordinated to six O atoms to form a TiO_6 octahedron. Upon the introduction of oxygen vacancy in pure TiO_2, there are three five-coordinated Ti atoms around the oxygen vacancy, as shown in Fig.2(b). The averaged optimized Ti−O distances around the oxygen vacancy are about 1.92 Å, which is slightly less than that of pure TiO_2 (1.98 Å). As shown in Fig.2 (c)−(f), when an oxygen vacancy is introduced in the V-C, V-N, Cr-C, and Cr-N pairs codoped antanse TiO_2, the oxygen vacancy prefers to the neighboring site of metal dopant, such as V or Cr atom. Then the n dopant is five-coordinated, and Ti atoms around the oxygen vacancy are also five-coordinated for the most stable configurations. In these optimized structures of codoped systems with oxygen vacancy, the V−C, V−N, Cr−C, and Cr−N distances are predicted to 1.71, 1.69, 1.65, and 1.81 Å, which are slightly different from these codoped without oxygen vacancy ($d_{V\text{-}C}$=1.78 Å, $d_{V\text{-}N}$=1.67 Å, $d_{Cr\text{-}C}$=1.64 Å, and $d_{Cr\text{-}N}$=1.61 Å), respectively. Note that the averaged Ti−O distance around the oxygen vacancy in these codoped TiO_2 systems just changes slightly (about 1.86 Å).

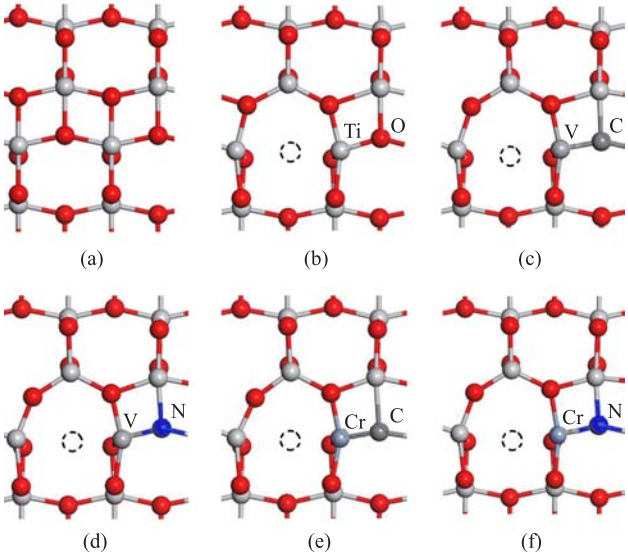

FIG. 2 Optimized structures of n-p codoped TiO_2 with oxygen vacancy (side view). (a) TiO_2, (b) O_v/TiO_2, (c) VC-O_v/TiO_2, (d) VN-O_v/TiO_2, (e) CrC-O_v/TiO_2, (f) CrN-O_v/TiO_2. The gray and red balls stand for Ti and O atoms, respectively. Oxygen vacancy and codoping pair are also labeled for clarity.

B. Electronic structure and band alignment

The spin-polarized band structures of these examined n-p codoped TiO_2 without and with oxygen vacancy at the most stable case are calculated and plotted in the left and right panels of Fig.3, respectively. Compared with pure antanse TiO_2, a n-p pair codoped TiO_2 ensures the creation of impurity bands within the band gap, which effectively narrows the band gap of TiO_2. For example, the effective band gaps of V-C, V-N, Cr-C, and Cr-N codoped TiO_2 are tuned to be 0.9, 2.4, 1.6, and 1.8 eV, respectively, which agree well with those previous theoretical reports [8]. To improve the photoelectrochemical (PEC) water splitting efficiency of TiO_2, band gap needs to be tuned to match the visible-light region, and the band-edge offset is engineered to maintain the redox performance at the same time. This implies that, to improve the reduction ability for hydrogen production, the position of the conduction band minimum (CBM) of the codoped TiO_2 should be kept as high as possible. In view of this requirement, the ability for H_2 production based on TiO_2 with n-p codoping pairs is not better than pure TiO_2 due to the downward shift of the CBM. Note that the intermediate bands mainly locate above the Fermi level, these empty intermediate bands contributed by n-p dopants act as the recombination centers for the photoinduced electrons and holes, then reduce the PEC efficiency of antanse TiO_2.

When an oxygen vacancy is introduced in the pure antanse supercell, the defect states, plotted with two

DOI:10.1063/1674-0068/28/cjcp1411196

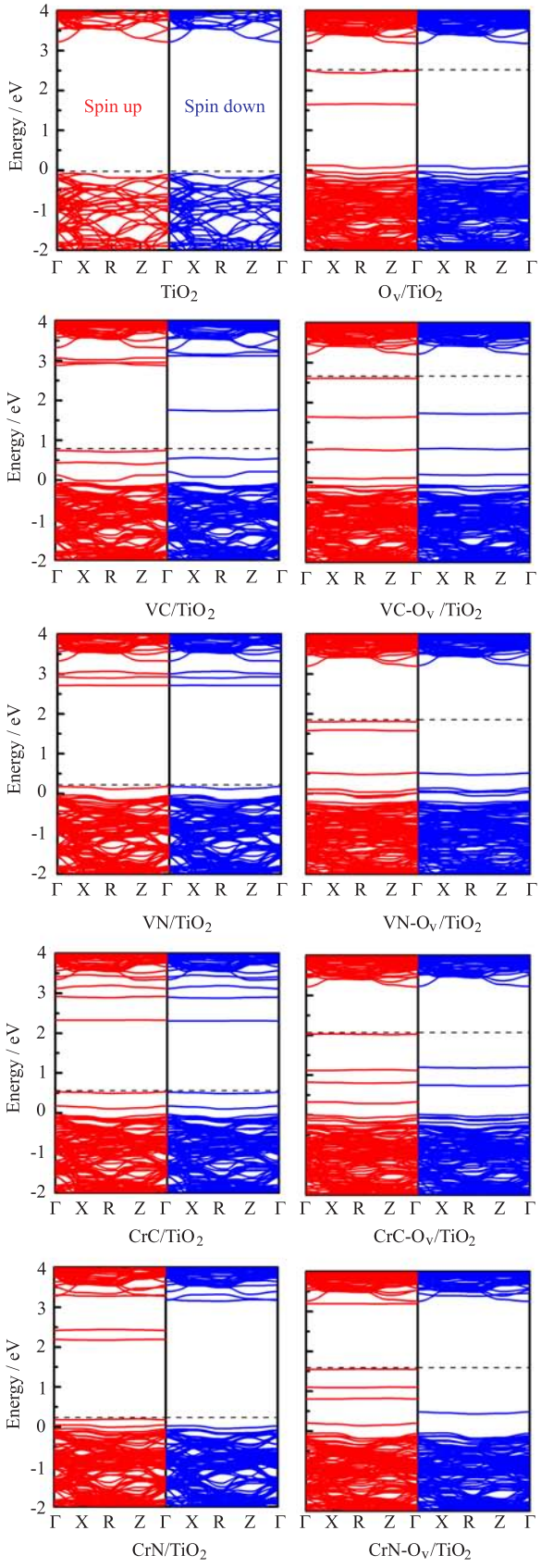

FIG. 3 Band structures of TiO_2 without and with oxygen vacancy. The dashed lines stand for the Fermi level.

red lines below the Fermi level about 1.6 and 2.5 eV in the right panel of Fig.3(a), are fully occupied, which are mainly contributed by Ti3d orbitals. It has been well established that the reduction of Ti^{4+} to Ti^{3+} occurs in TiO_2 with oxygen vacancy due to the charge imbalance. This observation indicates that the oxygen vacancy results in n-type semiconducting behaviors in TiO_2. As shown in the right panels of Fig.3 (b)−(e), it is clear that, upon the introduction of oxygen vacancy, the valent band maximum (VBM) increases significantly, compared to the n-p co-doped TiO_2 system, while the position of the CBM changes slightly. This observation is easy to understand. The presence of oxygen vacancy as well as the V-C, V-N, Cr-C, and Cr-N codoping pair in antanse TiO_2 breaks the crystal field of oxygen octahedra, lowers the symmetry and degeneration, which allows additional energy level splitting. Moreover, these unoccupied impurity bands in n-p codoped TiO_2 are filled, which is benefited for the reduction of recombination centers, and then improves the PEC performance of antanse TiO_2. On the other hand, the position of the CBM changes slightly upon the introduction of oxygen vacancy, which implies that the hydrogen production of water splitting processes is thermodynamically feasible for the n-p codoped TiO_2 with oxygen vacancy.

It is well known that the photoinduced electron transfer between the semiconductor and the adsorbates is dominated by the band energy positions of a semiconductor with respect to the redox potential of the adsorbed species on its surface dominate [32, 33]. Thermodynamically, to donate an electron to the vacant hole, the valence band potential of the semiconductor needs to be below the potential level of the donor dopants, while the conduction band potential of the semiconductor should be above the relevant potential level of the acceptor species [34, 35]. To evaluate the oxygen vacancy effect on the photocatalytic activity of the most preferred V−N codoped TiO_2, we illustrate the alignment of water reduction and oxidation potential with respect to the band edges of V-N codoped TiO_2 system in Fig.4. Here, the values of the VB edge and CB edge positions of the pure anatase TiO_2 with respect to the normal hydrogen electrode (NHE) potential are taken from the experimental values [36]. Clearly, we can observe the following main features: (i) TiO_2 has a strong reducing ability ascribed to its relative higher CBM (about 0.3 eV higher than the H^+/H_2 potential) as compared to the NHE potential, while the VBM is more positive (about 1.2 eV) than the O_2/H_2O potential. (ii) For TiO_2 with oxygen vacancy, the VBM shifts upward by 0.20 eV compared with pure TiO_2, but its water oxidation ability is still good. The CBM slightly shifts with respect to that of pure TiO_2. The main feature is that two occupied impurity bands appear within the band gap. (iii) The V-N codoped TiO_2 is not suitable for H_2 production since the impurity band appears within the band gap is unoccupied, which can act as

DOI:10.1063/1674-0068/28/cjcp1411196

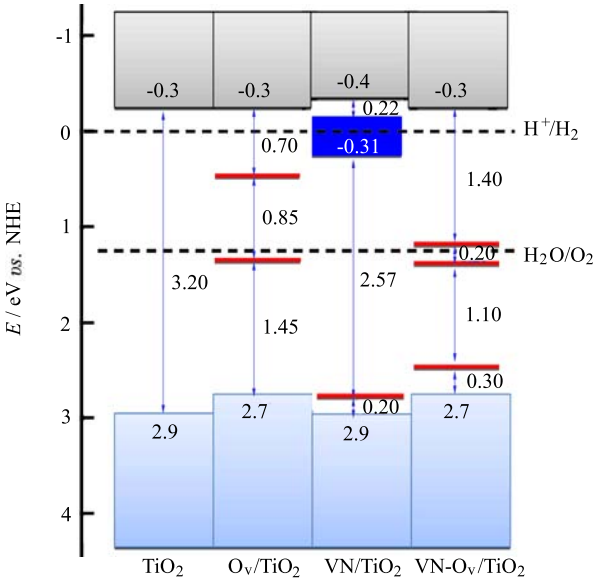

FIG. 4 The band edge alignment of the TiO_2, O_v/TiO_2, VN/TiO_2, and $VN\text{-}O_v/TiO_2$ with respect to the water reduction and oxidation potentials. Here, the gray and light blue regions stand for the CBs and VBs, while the localized and delocalized impurity bands are labeled with the narrow and broad lines, the blue and red bands stand for unoccupied and occupied states, respectively.

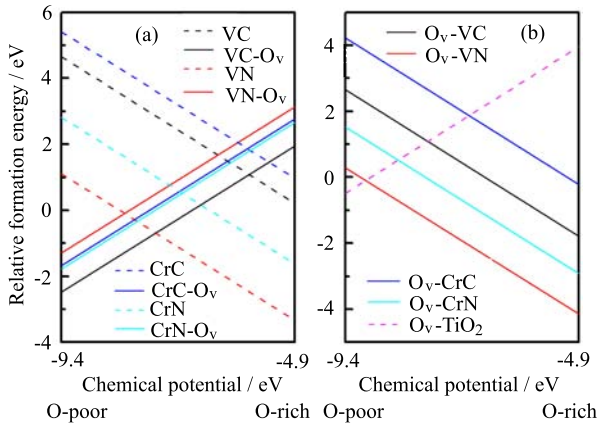

FIG. 5 The calculated relative formation energies of n-p codoped TiO_2 with oxygen vacancy as a function of the O-poor and O-rich chemical potentials. (a) Case 1. (b) Case 2.

the recombination centers of the photoinduced electrons and holes, and then reduce the PEC efficiency. (iv) For V-N codoped TiO_2 with oxygen vacancy, we find that it has the highest figure of merit for the PEC water splitting, because it not only does narrow the band gap, which is ideal for absorbing visible light, but also the impurity band is occupied, resulting in the reduction of recombination centers. Note that H_2 production are thermodynamically feasible for V-N codoped TiO_2 with oxygen vacancy under visible light.

C. Optimal growth condition

In search for the optimal growth condition in experiments, we examine the formation energies of the V-C, Cr-N, V-N, and Cr-C codoped TiO_2 systems with oxygen vacancy under O-poor and O-rich conditions. We examine two situations: TiO_2 is firstly codoped with n-p pairs, then oxygen vacancy is introduced (case 1); TiO_2 is firstly introduced with an oxygen vacancy, then the system is codoped with n-p pairs (case 2). The responding calculated results are shown in Fig.5. It is clear that the relative formation energies vary as a function of the chemical potentials of oxygen element. The formation energies are positive for the V-C and Cr-C codoped TiO_2 systems, which suggests that it is hard to introduce the V-C and Cr-C pairs into TiO_2, while it is possible to realize the V-N and Cr-N codoping in TiO_2 under O-rich condition. Interestingly, due to the negative formation energies for case 1, oxygen vacancy can be produced in the V-C, Cr-N, V-N, and Cr-C codoped TiO_2 systems under O-poor condition. For case 2, it is easier to codope V-C, Cr-N, V-N, and Cr-C pairs into TiO_2 with oxygen vacancy under O-rich condition. Fortunately, under O-poor condition, the formation energies for V-N codoped TiO_2 with oxygen vacancy are negative for both case 1 and case 2. This implies that this system is energetically favorable and can be easily achieved in experiments under the O-poor condition.

IV. CONCLUSION

We examine the effect of oxygen vacancy on the geometric and electronic structures of n-p pairs including V-C, V-N, Cr-C, and Cr-N codoped TiO_2 systems. Theoretical results show that oxygen vacancy prefers energetically to the neighboring site of metal dopant downward. The partially unoccupied impurity bands of n-p codoped systems can be filled due to the presence of oxygen vacancy, which results in the reduction of photoinduced carrier recombination. Among these examined V-N codoped systems, the band edge alignments in the V-N codoped TiO_2 with oxygen vacancy are desirable for hydrogen production via water-splitting. Moreover, oxygen vacancy is easily introduced in V-N codoped TiO_2 under O-poor condition. These theoretical findings are useful for understanding and explaining the related experimental observations, also are helpful for improving the PEC performance of codoped TiO_2.

V. ACKNOWLEDGMENTS

This work was supported by the National Natural Science Foundation of China (No.11034006, No.21273208, and No.21473168), the Anhui Provincial Natural Science Foundation (No.1408085QB26), the Fundamental Research Funds for the Central Universities, the China

DOI:10.1063/1674-0068/28/cjcp1411196

Postdoctoral Science Foundation (No.2012M511409), and the Supercomputing Center of Chinese Academy of Sciences, Shanghai and USTC Supercomputer Centers.

[1] X. Chen and S. S. Mao, Chem. Rev. **107**, 2891 (2007).
[2] X. Chen, S. Shen, L. Guo, and S. S. Mao, Chem. Rev. **110**, 6503 (2010).
[3] A. Fujishima, X. Zhang, and D. A. Tryk, Surf. Sci. Rep. **63**, 515 (2008).
[4] A. Kudo and Y. Miseki, Chem. Soc. Rev. **38**, 253 (2009).
[5] R. Asahi, T. Morikawa, T. Ohwaki, K. Aoki, and Y. Taga, Science **293**, 269 (2001).
[6] M. Grätzel, Nature (London) **414**, 338 (2001).
[7] Y. Gai, J. Li, S. S. Li, J. B. Xia, and S. H. Wei, Phys. Rev. Lett. **102**, 036402 (2009).
[8] W. Zhu, X. Qiu, V. Iancu, X. Q. Chen, H. Pan, W. Wang, N. M. Dimitrijevic, T. Rajh, H. M. Meyer, M. P. Paranthaman, G. M. Stocks, H. H. Weitering, B. Gu, G. Eres, and Z. Zhang, Phys. Rev. Lett. **103**, 226401 (2009).
[9] W. J. Yin, H. Tang, S. H. Wei, M. M. Al-Jassim, J. Turner, and Y. Yan, Phys. Rev. B **82**, 045106 (2010).
[10] S. U. M. Khan, M. Al-Shahry, and W. B. Jr. Ingler, Science **297**, 2243 (2002).
[11] Z. H. Lin, A. Orlov, R. M. Lambert, and M. C. Payne, J. Phys. Chem. B **109**, 20948 (2005).
[12] W. Choi, A. Termin, and M. R. Hoffmann, J. Phys. Chem. **98**, 13669 (1994).
[13] M. I. Litter, Appl. Catal. B **23**, 89 (1999).
[14] J. Tang, J. R. Durrant, and D. R. Klug, J. Am. Chem. Soc. **130**, 13885 (2008).
[15] J. Zhang, Y. Wu, M. Xing, S. A. K. Leghari, and S. Sajjad, Energy Environ. Sci. **3**, 715 (2010).
[16] J. Nowotny, T. Bak, M. K. Nowotny, and L. R. Sheppard, Int. J. Hydrogen Energy, **32**, 2630 (2007).
[17] J. Nowotny, T. Bak, M. K. Nowotny, and L. R. Sheppard, Int. J. Hydrogen Energy **32**, 2609 (2007).
[18] M. K. Nowotny, L. R. Sheppard, T. Bak, and J. Nowotny, J. Phys. Chem. C **112**, 5275 (2008).
[19] G. Pacchioni, ChemPhysChem **4**, 1041 (2003).
[20] S. Polarz, J. Strunk, V. Ischenko, M. W. E. van den Berg, O. Hinrichsen, M. Muhler, and M. Driess, Angew. Chem. Int. Ed. **45**, 2965 (2006).
[21] Z. Zhang, O. Bondarchuk, J. M. White, B. D. Kay, and Z. Dohnalek, J. Am. Chem. Soc. **128**, 4198 (2006).
[22] X. Pan, M. Q. Yang, X. Fu, N. Zhang, and Y. J. Xu, Nanoscale **5**, 3601 (2013).
[23] G. Kresse and J. Hafner, Phys. Rev. B **47**, 558 (1993).
[24] P. E. Blöchl, Phys. Rev. B **50**, 17953 (1994).
[25] J. P. Perdew, K. Burke, and M. Ernzerhof, Phys. Rev. Lett. **77**, 3865 (1996).
[26] H. J. Monkhorst and J. D. Pack, Phys. Rev. B **13**, 5188 (1976).
[27] V. I. Anisimov, J. Zaanen, and O. K. Andersen, Phys. Rev. B **44**, 943 (1991).
[28] V. I. Anisimov, F. Aryasetiawan, and A. I. Lichtenstein, J. Phys.: Condens. Matter **9**, 767 (1997).
[29] X. Du, Q. Li, H. Su, and J. Yang, Phys. Rev. B **74**, 233201 (2006).
[30] J. Wang, H. Sun, J. Huang, Q. Li, and J. Yang, J. Phys. Chem. C **118**, 7451 (2014).
[31] J. Wang, Q. Meng, J. Huang, Q. Li, and J. Yang, J. Chem. Phys. **140**, 174705 (2014).
[32] Y. Qu and X. Duan, Chem. Soc. Rev. **42**, 2568 (2013).
[33] P. Liao and E. A. Carter, Chem. Soc. Rev. **42**, 2401 (2013).
[34] A. L. Linsebigler, G. Lu, and J. T. Yates, Chem. Rev. **95**, 735 (1995).
[35] B. Ohtani, Phys. Chem. Chem. Phys. **16**, 1788 (2014).
[36] Y. Xu and M. A. A. Schoonen, Am. Mineral. **85**, 543 (2000).

DOI:10.1063/1674-0068/28/cjcp1411196